Discovery of a giant H I tail in the galaxy group HCG 44

Paolo Serra,[1]★ Bärbel Koribalski,[2] Pierre-Alain Duc,[3] Tom Oosterloo,[1,4]
Richard M. McDermid,[5] Leo Michel-Dansac,[6] Eric Emsellem,[6,7]
Jean-Charles Cuillandre,[8] Katherine Alatalo,[9] Leo Blitz,[9] Maxime Bois,[10]
Frédéric Bournaud,[3] Martin Bureau,[11] Michele Cappellari,[11] Alison F. Crocker,[12]
Roger L. Davies,[11] Timothy A. Davis,[7] P. T. de Zeeuw,[7,13] Sadegh Khochfar,[14]
Davor Krajnović,[7] Harald Kuntschner,[7] Pierre-Yves Lablanche,[6,7]
Raffaella Morganti,[1,4] Thorsten Naab,[15] Marc Sarzi,[16] Nicholas Scott,[17]
Anne-Marie Weijmans[18]† and Lisa M. Young[19]

[1]*Netherlands Institute for Radio Astronomy (ASTRON), Postbus 2, 7990 AA Dwingeloo, the Netherlands*
[2]*Australia Telescope National Facility, CSIRO Astronomy and Space Science, PO Box 76, Epping, NSW 1710, Australia*
[3]*Laboratoire AIM Paris-Saclay, CEA/IRFU/SAp-CNRS-Université Paris Diderot, 91191 Gif-sur-Yvette Cedex, France*
[4]*Kapteyn Astronomical Institute, University of Groningen, Postbus 800, 9700 AV Groningen, the Netherlands*
[5]*Gemini Observatory, Northern Operations Centre, 670 N. A'ohoku Place, Hilo, HI 96720, USA*
[6]*Centre de Recherche Astrophysique de Lyon and Ecole Normale Supérieure de Lyon, Université Lyon 1, Observatoire de Lyon,*
9 avenue Charles André, F-69230 Saint-Genis Laval, France
[7]*European Southern Observatory, Karl-Schwarzschild-Str. 2, 85748 Garching, Germany*
[8]*Canada–France–Hawaii Telescope Corporation, 65-1238 Mamalahoa Hwy., Kamuela, HI 96743, USA*
[9]*Department of Astronomy, Campbell Hall, University of California, Berkeley, CA 94720, USA*
[10]*LERMA, Observatoire de Paris and CNRS, 61 Avenue de l'Observatoire, 75014 Paris, France*
[11]*Sub-Department of Astrophysics, Department of Physics, University of Oxford, Denys Wilkinson Building, Keble Road, Oxford OX1 3RH*
[12]*Department of Astronomy, University of Massachusetts, Amherst, MA 01003, USA*
[13]*Sterrewacht Leiden, Leiden University, Postbus 9513, 2300 RA Leiden, the Netherlands*
[14]*Max-Planck Institut für extraterrestrische Physik, PO Box 1312, D-85478 Garching, Germany*
[15]*Max-Planck-Institut für Astrophysik, Karl-Schwarzschild-Str. 1, 85741 Garching, Germany*
[16]*Centre for Astrophysics Research, University of Hertfordshire, Hatfield, Herts AL1 9AB*
[17]*Centre for Astrophysics and Supercomputing, Swinburne University of Technology, Hawthorn, VIC 3122, Australia*
[18]*Dunlap Institute for Astronomy & Astrophysics, University of Toronto, 50 St. George Street, Toronto, ON M5S 3H4, Canada*
[19]*Physics Department, New Mexico Institute of Mining and Technology, Socorro, NM 87801, USA*

ABSTRACT

We report the discovery of a giant H I tail in the intragroup medium of HCG 44 as part of the ATLAS^{3D} survey. The tail is ~300 kpc long in projection and contains ~5×10^8 M$_\odot$ of H I. We detect no diffuse stellar light at the location of the tail down to ~28.5 mag arcsec^{-2} in g band. We speculate that the tail might have formed as gas was stripped from the outer regions of NGC 3187 (a member of HCG 44) by the group tidal field. In this case, a simple model indicates that about 1/3 of the galaxy's H I was stripped during a time interval of <1 Gyr. Alternatively, the tail may be the remnant of an interaction between HCG 44 and NGC 3162, a spiral galaxy now ~650 kpc away from the group. Regardless of the precise formation mechanism, the detected H I tail shows for the first time direct evidence of gas stripping in HCG 44. It also highlights that deep H I observations over a large field are needed to gather a complete census of this kind of events in the local Universe.

Key words: galaxies: evolution – galaxies: groups: general – galaxies: groups: individual: HCG 44 – galaxies: interactions – galaxies: ISM.

★ E-mail: serra@astron.nl
† Dunlap Fellow.

1 INTRODUCTION

Deep observations of neutral hydrogen (H I) around galaxies often reveal faint gaseous distributions which do not trace galaxies' stellar light. Known cases include extremely large H I discs and rings around both late-type galaxies (e.g. Krumm & Burstein 1984; Meurer et al. 1996; Koribalski & López-Sánchez 2009) and early-type galaxies (e.g. van Driel & van Woerden 1991; Morganti et al. 2006; Oosterloo et al. 2007; Serra et al. 2012), tidal tails around merger remnants (e.g. Schiminovich et al. 1994; Koribalski, Gordon & Jones 2003; Duc et al. 2011), tidal and ram-pressure tails in galaxy groups and clusters (e.g. Verheijen & Zwaan 2001; Davies et al. 2004; Oosterloo & van Gorkom 2005; English et al. 2010; Scott et al. 2012; Serra et al. 2012), gas accretion signatures (Sancisi et al. 2008, and references therein) and objects whose origin is still debated (e.g. Schneider et al. 1983; Thilker et al. 2009; Michel-Dansac et al. 2010). These systems carry invaluable information on the way galaxies assemble their stellar mass and accrete and lose gas in different environments.

Neutral hydrogen distributions revealing ongoing tidal interaction, galaxy merging and gas stripping are particularly common in groups of galaxies (e.g. van der Hulst 1979; Verdes-Montenegro et al. 2001; Kern et al. 2008; Freeland, Stilp & Wilcots 2009; see also Hibbard et al. 2001, and references therein). The observation of these processes *in action* suggests that the morphology and gas content of galaxies can undergo substantial evolution inside a group. In fact, group processes might be a major driver of the morphology–density relation (Dressler 1980; Postman & Geller 1984; for a discussion of the role of groups in determining this relation see e.g. Wilman et al. 2009; Bekki & Couch 2011; Cappellari et al. 2011b) and of the decrease of galaxies' H I content with increasing environment density (e.g. Verdes-Montenegro et al. 2001; Kilborn et al. 2009; Rasmussen et al. 2012a; Serra et al. 2012).

Strong indications of the importance of group processes come from a combination of optical and H I results presented recently as part of the ATLAS[3D] survey (Cappellari et al. 2011a). First, the fraction of fast rotating early-type galaxies increases (and the fraction of spiral galaxies decreases) with environment density following a surprisingly tight log–linear relation, which is steeper and better defined when the density is measured on a group-like scale (defined by the distance from the third closest neighbour) rather than a cluster-like scale (tenth neighbour; Cappellari et al. 2011b). Secondly, the H I morphology of gas-rich early-type galaxies appears to be strongly related to environment density when the latter is measured on a group-like scale (Serra et al. 2012). Large, regular, settled H I distributions are typical in poor environments (where the distance from the third neighbour is larger than a few Mpc). More disturbed distributions are typical in galaxy groups and may be revealing the processes responsible for the morphology–density relation.

We note that understanding group processes is important to understand galaxy properties over a broad range of *large-scale* environment densities. On one hand, in a Λ cold dark matter Universe galaxy clusters grow by accretion of groups of (rather than isolated) galaxies, and pre-processing in groups may be important to shape the properties of galaxies living in clusters at redshift zero. On the other hand, even inside large-scale voids galaxies live clustered in small groups and their evolution is to some extent driven by tidal interactions and merging (Szomoru et al. 1996; Kreckel et al. 2012).

Within this context, stripping of gas from galaxies in groups plays a key role. Although direct detection of stripped gas has been possible in a number of groups (see references above), in
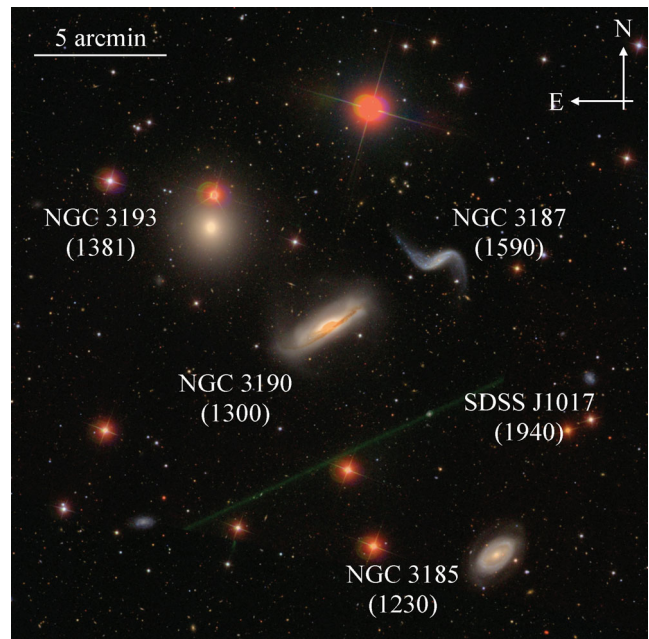

Figure 1. Sloan Digital Sky Survey (SDSS) optical colour image of HCG 44 (Data Release 8). The image covers an area of 0.4×0.4 deg^2. We obtained the image at http://skyserver.sdss3.org/dr8/en/tools/chart/chart.asp. For each galaxy we indicate in parenthesis under the galaxy name the heliocentric recessional velocity in km s^{-1} (see Table 1).

many other systems galaxies are found to be H I deficient but no intragroup H I is detected. From an observational point of view the main challenge is that the stripped gas can diffuse quickly in the group medium (in about a group crossing time). It therefore reaches low column densities, requiring high sensitivity, and spreads over large areas, requiring observations over a large field. At the moment it is therefore unclear how ubiquitous gas stripping is in groups and, in more quantitative terms, what fraction of the original H I mass of a galaxy can be stripped and on what time-scale. These estimates are needed to understand the importance of gas stripping relative to other processes which may play a role in determining the morphology–density relation, such as the decrease of the cold-gas accretion rate in denser environments.

In this paper, we report the discovery of a giant H I tail in the galaxy group HCG 44 as part of the ATLAS[3D] survey. We summarize the properties of the group in Section 2, describe radio and optical observations in Section 3, present and discuss the results in Sections 4 and 5, and draw conclusions in Section 6.

2 HICKSON COMPACT GROUP 44

HCG 44 is a compact group at a distance of ∼25 Mpc (see below) hosting four galaxies of comparable magnitude within an area of ∼15 × 15 arcmin^2 (Fig. 1; Hickson 1982). The two galaxies in the centre of the figure, NGC 3187 and NGC 3190,[1] exhibit signs of tidal interaction. The former is a blue, late-type spiral with long tails pointing ∼90° away from the plane of the galaxy. The latter is an earlier type system with a disturbed morphology and a prominent dust lane. Vorontsov-Velyaminov (1959) groups these galaxies together in the object VV 307 (later catalogued as

---

[1] Some authors refer to this galaxy as NGC 3189. According to the NASA Extragalactic Database NGC 3189 is the south-western side of NGC 3190.

Table 1. Galaxies in the HCG 44 field.

Galaxy	v_{hel} (km s^{-1})	Distance (Mpc)	Method	Reference
(1)	(2)	(3)	(4)	(5)
NGC 3185	1230	20 ± 5	TF	a
NGC 3187	1590	26 ± 10	TE	b
NGC 3190	1300	24 ± 5	SNIa	c, d, e, f, g, h, i
NGC 3193	1381	34 ± 3	SBF	j
SDSS J1017	1940	29	HF	This work

Columns are listed as follows. (1) Galaxy name. (2) Heliocentric velocity measured from the H I data discussed in this paper except for NGC 3193, for which we use the value given by Cappellari et al. (2011a). (3) Redshift-independent distance for all galaxies except SDSS J1017, for which we assume Hubble flow (see below). Error bars are taken from the references in column 5 except for NGC 3190, for which we give the range of distances obtained by different groups who studied the two SNIa 2002bo and 2002cv. (4) Method used to determine the distance: TF = Tully–Fisher relation corrected for Malmquist bias; TE = Tully estimate; SBF = surface brightness fluctuation corrected for Malmquist bias; HF = Hubble flow with $h = 0.73$ after correction for Virgo infall by $+200$ km s^{-1}. (5) References for the distance estimate: (a) Springob et al. (2009); (b) Tully (1988); (c) Reindl et al. (2005); (d) Wang et al. (2006); (e) Elias-Rosa et al. (2008); (f) Takanashi, Doi & Yasuda (2008); (g) Wood-Vasey et al. (2008); (h) Mandel et al. (2009); (i) Amanullah et al. (2010); and (j) Blakeslee et al. (2001).

Arp 316), suggesting that they are interacting. The early-type galaxy to the north-east, NGC 3193, is very close in projection to these two galaxies and has regular morphology. To the south-west, NGC 3185 is a barred galaxy with a warped, star-forming outer ring. In addition to these four galaxies listed in the original Hickson (1982) catalogue, the much smaller galaxy SDSS J101723.29+214757.9 (hereafter SDSS J1017) might be at larger distance (see below), while the small blue galaxy in the south-east corner is definitely a background object based on its Sloan Digital Sky Survey (SDSS) redshift of 0.014.

The group membership is not well established. Table 1 lists recessional velocity and distance estimates of the galaxies mentioned above. NGC 3185, NGC 3190 and NGC 3193 have comparable velocities. Relative to these, the velocity of NGC 3187 seems too large for such a small group. SDSS J1017 has even higher velocity, casting doubts on its membership.

Redshift-independent distance estimates of individual galaxies are also puzzling. Taken at face value, the distance of NGC 3193 would put it in the background, as suggested also by Aguerri et al. (2006) based on the non-detection of planetary nebulae in this galaxy. However, error bars on individual distance measurements are large and systematic effects may be important. For example, the two Type Ia supernovae (SNeIa) in NGC 3190 (see table) are extremely obscured and dust corrections are substantial. Furthermore, NGC 3185 has a warp and this would cause a systematic error on the Tully–Fisher distance based on single-dish H I data.

In this paper, we do not attempt to resolve the issue of galaxy distances and group membership. Instead, we assume that all galaxies labelled in Fig. 1 belong to the group with the exception of SDSS J1017, which we consider as a background object based on its large recessional velocity. We assume that the group is at a distance of $d_{HCG44} = 25$ Mpc. At this distance 15 arcmin correspond to $\sim$110 kpc.

We note that HCG 44 is part of a loose overdensity which includes 10 to 16 bright galaxies depending on the grouping criterion

(see group 58 in Geller & Huchra 1983 and group 194 in Garcia 1993). Galaxies in this overdensity have recessional velocity between $\sim$1100 and $\sim$1500 km s^{-1} and are distributed over a sky area of about 5×3 deg^2, which corresponds to 2.2×0.9 Mpc^2 at the distance of HCG 44. Therefore, galaxies in this region are relatively distant from each other (each of them occupies on average 0.6 deg$^2 \sim 0.1$ Mpc^2). In comparison, the galaxy number density within HCG 44 is 10 times larger, and this group stands out clearly as a strong and compact overdensity on top of the loose group.

The H I properties of HCG 44 have been studied by Williams & Rood (1987) using the Arecibo telescope, Williams, McMahon & van Gorkom (1991) and Verdes-Montenegro et al. (2001) with Very Large Array (VLA) data, van Driel et al. (2001) with the Nançay telescope, and Borthakur, Yun & Verdes-Montenegro (2010) using the Green Bank Telescope (GBT). These studies agree that galaxies in the group (all detected in H I except NGC 3193, which is claimed to be detected by van Driel et al. 2001 only) are gas poor relative to similar objects in the field. Verdes-Montenegro et al. (2001) estimate the detected H I mass to be just $\sim$40 per cent of the expected value for NGC 3187 and $\sim$10 per cent for NGC 3185 and NGC 3190 (we revisit these estimates in Section 4.2). Borthakur et al. (2010) report the detection of some of the missing gas as they find excess H I emission in the GBT spectrum[2] compared to the total VLA spectrum. Based on the strong similarity between the GBT and VLA H I profiles, they suggest that the excess gas is dynamically similar to the H I detected by the VLA within individual galaxies in the group.

We observed HCG 44 in H I as part of the multiwavelength ATLAS^{3D} survey (Cappellari et al. 2011a). The H I observations of this survey were carried out with the Westerbork Synthesis Radio Telescope (WSRT) and presented in Serra et al. (2012). Those observations revealed a few small gas clouds around HCG 44. Serra et al. (2012) argue that the distribution of the clouds on the sky and in velocity is suggestive of a long, intragroup H I tail – the detected clouds being the densest clumps along the hypothetical tail. Here we present new, deeper WSRT observations performed as part of the ATLAS^{3D} project to detect the H I tail itself.

3 OBSERVATIONS

3.1 H I interferometry

We observed HCG 44 for 6×12 h with the WSRT. We pointed the telescope at $\alpha_{J2000} = 10^h18^m54^s.19$, $\delta_{J2000} = 21^d59^m30^s.5$, which is a position between NGC 3193 and one of the H I clouds detected by Serra et al. (2012). We reduced the data in a standard way using the WSRT pipeline developed by Serra et al. (2012). The H I cube used for our analysis is made using robust $= 0$ weighting and 30 arcsec full width at half-maximum (FWHM) tapering. This results in a beam major and minor axis of 53.0 arcsec and 32.7 arcsec, respectively (PA $= 6^\circ.5$; the beam axes correspond to 6.4 and 4.0 kpc at the adopted distance, respectively). The cube has velocity resolution of 16 km s^{-1} after Hanning smoothing. The noise is $\sigma = 0.22$ mJy beam^{-1} in each channel, which corresponds to a formal 5σ H I column density sensitivity of 1.1×10^{19} cm^{-2} per resolution element.

We use the source finder described in Serra et al. (2012) to detect emission in the H I cube. The finder looks for emission in the original cube and in cubes at different resolutions on the sky and/or in velocity. It flags all voxels above $+n\sigma$ and all voxels below $-n\sigma$ as

---

[2] The GBT beam is $\sim$9 arcmin.

emission and performs basic size filtering to reduce the noise in the mask at each resolution. Here we use Gaussian filters of FWHM 25 and 50 arcsec on the sky and top-hat filters of width 16, 32, 64, 128, 256 and 384 km s^{-1} in velocity, and adopt $n = 3$. We use the resulting mask to build the total-H I image (which we then correct for the primary beam of the WSRT) and the H I velocity field (intensity-weighted mean) shown in Section 4. All H I flux and mass values reported in this paper are measured from the total-H I image and are therefore corrected for the primary beam.

3.2 Optical imaging

Deep optical imaging of HCG 44 was obtained with the MegaCam camera mounted on the Canada–France–Hawaii Telescope (CFHT). These observations were taken as part of the ATLAS^{3D} project (Cappellari et al. 2011a) with the goal of studying early-type galaxies' morphological fine-structure as a relic of their formation (Duc et al. 2011). We observed the HCG 44 field for 7×345 s in both g and r band applying offsets of $\sim$30 arcmin between consecutive exposures. The seeing was 0.9 and 1.2 arcsec in g and r band, respectively. We refer to Duc et al. (2011) for a full description of the observations and data reduction. We note here that the observing strategy and data reduction procedures (ELIXIR-LSB software; Cuillandre et al., in preparation) were chosen to detect stellar structures reaching $\sim$28.5 mag arcsec^{-2} in g band. However, the surface brightness sensitivity may vary from field to field (and within a given field), and we discuss the sensitivity of our image in more detail in the following section.

4 RESULTS

4.1 H I in the intragroup medium

Fig. 2 shows H I constant-column-density contours overlaid on the g-band CFHT/MegaCam image of HCG 44. The main result of our new observation is the detection of a long H I tail north of NGC 3193 (hereafter T_N), which is contained in the large, dashed red circle in the figure. The tail consists of a low-column-density, $\sim$20-arcmin-long component oriented north-west to south-east and a less massive, southern extension. The latter is revealed by two small clouds aligned north-east to south-west in the direction of NGC 3193. We also confirm the Serra et al. (2012) detection of a smaller H I complex south-east of NGC 3193 (hereafter C_S), indicated by the small, dashed red circle in the figure.

The tail T_N has no diffuse optical counterpart down to the surface brightness sensitivity of the deep image shown in Fig. 2 (the same result is obtained inspecting the r-band image). In Section 3.2, we mentioned that the generic sensitivity of the CFHT/MegaCam images taken as part of the ATLAS^{3D} project is $\sim$28.5 mag arcsec^{-2} in g band. In this particular case T_N lays on a relatively clean region of the image, which shows no large-scale noise variations or bright sources with the exception of two stars in the southern part of the tail. The noise level in this region (excluding the two stars) corresponds to a 1.5σ detection limit of 28.4 mag arcsec^{-2} within a circular aperture of radius equal to the seeing, consistent with the generic value given above. Such low detection level per resolution element is sufficient considering that we are looking for emission over a scale of many arcminutes.

Fig. 3 shows the velocity field of the detected H I. We find a smooth variation of H I recessional velocity along T_N. This is shown more clearly by the position–velocity diagram in Fig. 4, which is drawn along the path indicated by the black solid line in Fig. 3. The clouds detected by Serra et al. (2012) and mentioned in Section 1 are therefore just the tip of the iceberg of a large, coherent, gas distribution, as suggested in that paper. Gas in both T_N and C_S is detected at velocities comparable to that of individual galaxies in HCG 44, suggesting that the tails are parts of the group. T_N has a total projected length of $\sim$220 kpc at the assumed distance $d_{HCG\ 44} = 25$ Mpc.

Table 2 lists the H I flux of all detected objects shown in Fig. 2. Table 2 also shows the fractional contribution f(H I) of each object to the total-H I flux of the group. Assuming that all galaxies in HCG 44 and the intragroup gas are roughly at the same distance, we conclude that H I in T_N and C_S amounts to $\sim$20 per cent of the total neutral hydrogen mass of the compact group. This is as much H I as that found in NGC 3190 and almost half the H I mass of NGC 3187. At the assumed distance d_{HCG44} we estimate an H I mass of 4.1×10^8 and 1.2×10^8 M$_\odot$ for T_N and C_S, respectively.

We note that T_N stretches beyond the FWHM of WSRT's primary beam, which is 0°.6 at the observing frequency of our data. Therefore, it is possible that the gaseous tail is actually longer than shown in Fig. 2 and we stop detecting H I because of a decrease in the telescope response. To check whether this is the case we make a natural-weighting H I cube from our WSRT data. This weighting scheme produces a cube with very patchy noise and poorer image quality, but the sensitivity is better than that of the main cube used in this study. Fig. 5 shows a channel of the natural-weighting cube at velocity 1248 km s^{-1} suggesting indeed that some additional H I emission may exist north-west of T_N.

The existence of a north-western extension of T_N is confirmed by data taken as part of the H I Parkes All Sky Survey (HIPASS; Barnes et al. 2001). The HIPASS cube[3] of this sky area has noise of $\sim$15 mJy beam^{-1}, velocity resolution 18 km s^{-1} and beam FWHM 15.5 arcmin. The formal 5σ sensitivity per resolution element is 1.7×10^{18} cm^{-2} for gas filling the beam. We run the source finder described in Section 3.1 on the cube and show contours of the detected H I in Fig. 6 overlaid on an SDSS g-band image (we also show the lowest WSRT H I contour; see Fig. 2).

The figure shows two clear HIPASS detections at the location of HCG 44 and NGC 3162 (a spiral galaxy $\sim$1°.5 north-west of HCG 44). Both detections are listed in the northern HIPASS catalogue by Wong et al. (2006) – objects HIPASS J1017+21 and HIPASS J1013+22, respectively. The main part of T_N is visible only at a tentative level in HIPASS (partly because the cube contains many artefacts) and the HIPASS contours in Fig. 6 do not show it. On the other hand, the HIPASS cube reveals additional emission (not included in the catalogue of Wong et al. 2006) just north-west of T_N, which was missed by our WSRT data because of its large distance from the pointing centre. The velocity of this emission is consistent with the velocity field shown in Fig. 3. Including this emission, the length of T_N becomes $\sim$300 kpc and its mass 5.2×10^8 M$_\odot$. This result is confirmed by the newly reduced HIPASS data, which have significantly lower noise level and many less artefacts (Calabretta et al., in preparation). In the new data the full tail is detected clearly (HIPASS team, private communication).

Another interesting aspect revealed by the HIPASS data is that the H I tail stretches towards and possibly connects with NGC 3162 (this galaxy was already detected in H I by e.g. van Driel et al. 2001). NGC 3162, whose optical image we show in the inset of Fig. 6, has
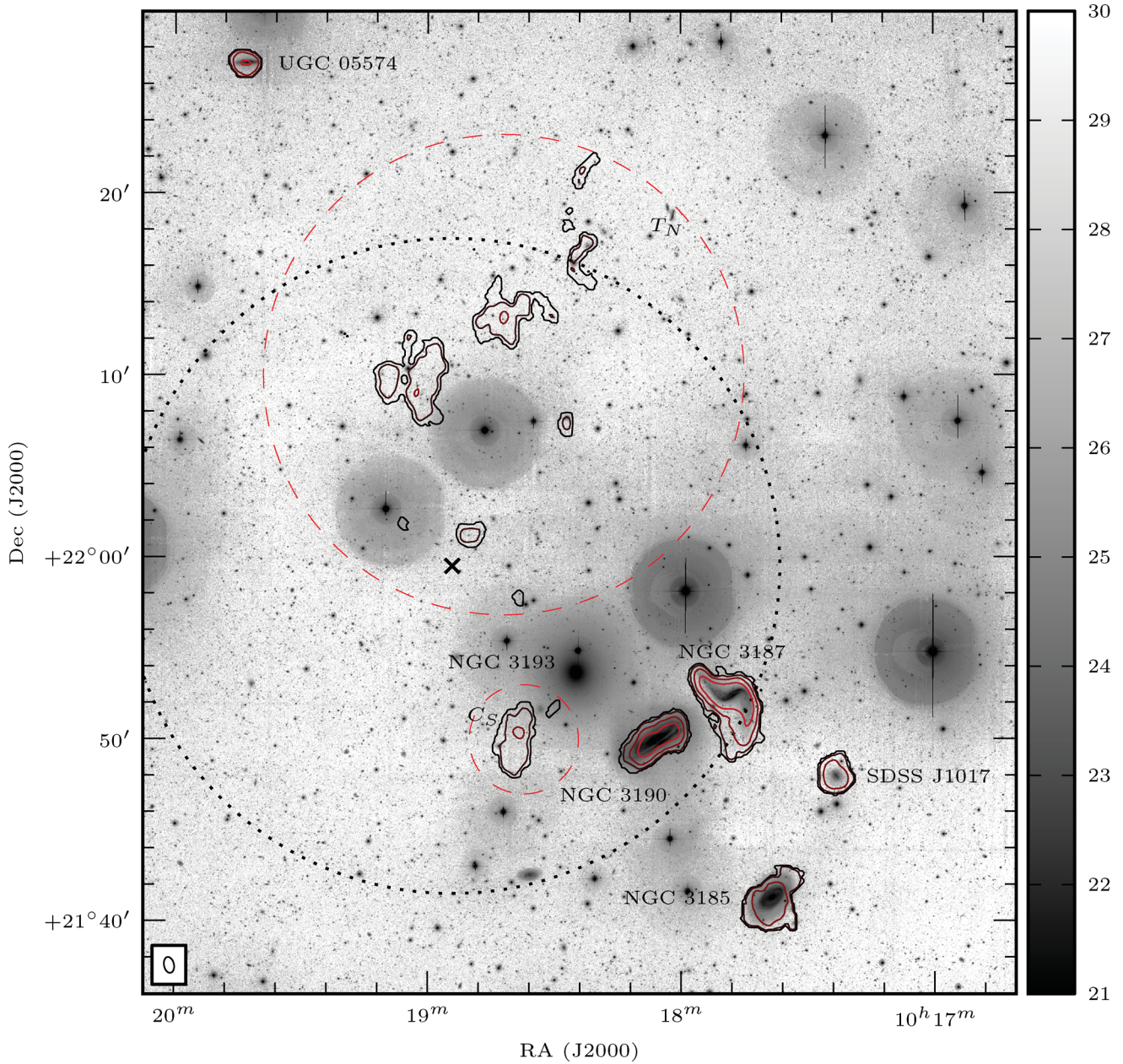
---

[3] Available at http://www.atnf.csiro.au/research/multibeam/release.

Figure 2. Constant-column-density H I contours overlaid on the *g*-band CFHT/MegaCam image. The colour bar on the right is in mag arcsec^{-2}. Contours represent $N(\text{H I}) = 1.0 \times 10^{19} \times 3^n$ cm^{-2} ($n = 0, 1, 2, 3$). Contours are coloured black to red, faint to bright. The black cross indicates the pointing centre of our WSRT observation and the dotted, black circle indicates the primary beam of the WSRT. Large and small dashed, red circles indicate the location of T_N and C_S, respectively (see text). The beam of the H I image is shown on the bottom-left corner. Note that UGC 05574 (to the north-east) and SDSS J1017 (to the south-west) are not members of HCG 44.

H I recessional velocity of 1300 km s^{-1}, comparable to that of HCG 44 members, and is at a projected distance of ∼650 kpc from HCG 44 assuming the distance d_{HCG44} along the line of sight. We discuss this finding in Section 5.

4.2 H I in galaxies: comparison to previous studies

All gas-rich galaxies in Fig. 2 were already known to host H I. Williams et al. (1991) observed this group with the VLA. They report H I fluxes systematically larger than those in Table 2. Namely, the flux of NGC 3185, NGC 3187, NGC 3190 and SDSS J1017 is

a factor of 1.7, 1.3, 1.3 and 2.4 larger than our value, respectively.[4] For NGC 3185 and SDSS J1017 part of the difference may be due to the better column density sensitivity of the VLA data relative to

[4] These factors include a correction of the VLA fluxes for the primary beam of that telescope, which was not applied by Williams et al. (1991). The primary-beam correction is of ∼10 per cent for NGC 3185 and SDSS J1017, while it is negligible for the other two objects. Note that the VLA flux values are consistent with those reported by Williams & Rood (1987) using Arecibo data. They are adopted by Verdes-Montenegro et al. (2001) in their H I study of Hickson compact groups. They are 5–20 per cent larger than values in van Driel et al. (2001), which have however large uncertainty.
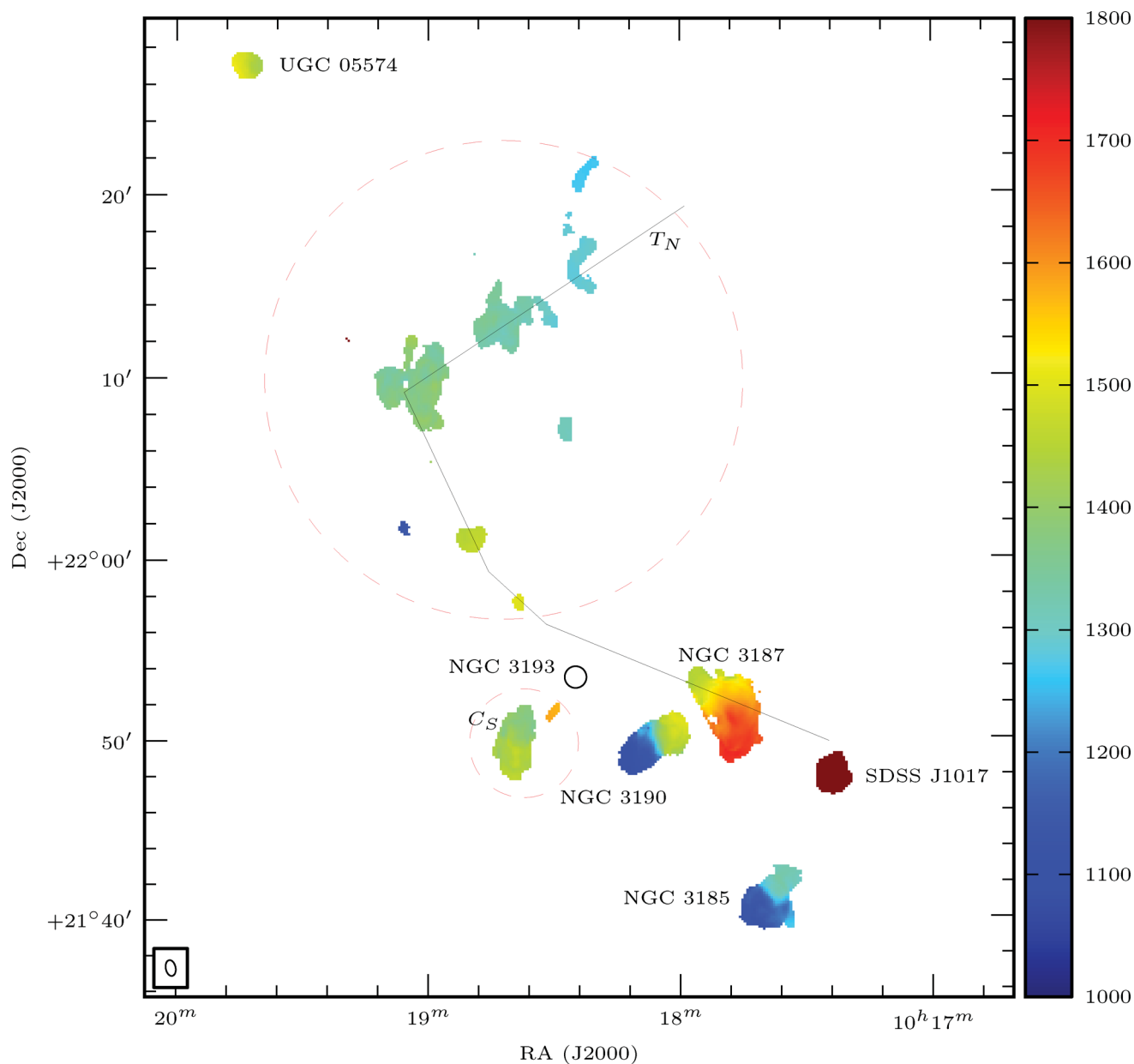
Figure 3. Velocity field of the detected H I. The colour bar on the right is in km s^{-1}. Large and small dashed, red circles indicate the location of T_N and C_S, respectively. The black open circle indicates the position of NGC 3193, whose recessional velocity from optical spectroscopy is 1381 km s^{-1}. The beam of the H I image is shown on the bottom-left corner. The black solid line is the path used to draw the position–velocity diagram shown in Fig. 4.

our WSRT data (by a factor of ∼1.7; these galaxies are relatively far from the WSRT pointing centre as shown in Fig. 2). On the contrary, our data are slightly more sensitive at the location of NGC 3187 and NGC 3190 (10–20 per cent) so at least some of the flux difference must have a different cause.

Flux calibration is not the reason of this discrepancy as we have verified that our calibration is consistent with that of Williams et al. (1991) within ±10 per cent. Instead, we do find a relevant difference in the way we build the total-H I image. In our study we use the source finder of Serra et al. (2012), which includes in the H I image both positive and negative noise peaks (see Section 3.1). On the contrary, Williams et al. (1991) select only voxels above +1.5σ. This introduces a positive bias in the total-H I flux. Indeed, if we implement their detection criterion in our source finder we obtain fluxes a factor of 1.5, 1.1, 1.2 and 1.3 larger for the four galaxies

mentioned above, respectively. This accounts at least partially for the difference in H I flux. Remaining differences may be explained by the better sensitivity of the VLA data at the location of NGC 3185 and SDSS J1017 (see above) and by the higher noise level of the VLA data at the location of NGC 3187 and NGC 3190, which would imply a higher level of the bias under discussion.

The H I morphology of galaxies in Fig. 2 is in agreement with the image presented by Williams et al. (1991). The main addition of our deeper image (besides the detection of T_N and C_S) is a faint extension of the southern H I warp in NGC 3187. Furthermore, we set a column density limit of ∼2 × 10^{19} cm^{-2} on the H I bridge between NGC 3185 and NGC 3190, which was tentatively suggested by Williams et al. (1991) based on the VLA data (this limit takes into account that the two galaxies lay around the half-power point of the WSRT primary beam).

Table 2. H I detected with the WSRT in HCG 44.

Object	F(H I) (Jy km s^{-1})	f(H I)	M(H I) ($\times 10^8 M_\odot$)
(1)	(2)	(3)	(4)
T_N	2.79	0.15	4.1
C_S	0.82	0.05	1.2
NGC 3185	2.11	0.12	3.1
NGC 3187	8.22	0.46	12.0
NGC 3190	4.00	0.22	5.8
Galaxies not members of HCG 44			
SDSS J1017	1.03	–	2.0
UGC 05574	0.84	–	1.1

Columns are listed as follows. (1) Object name. (2) Total H I flux. (3) Fraction of the total H I flux of HCG 44. (4) H I mass assuming a distance of $d_{HCG\,44} = 25$ Mpc for galaxies in HCG 44, and Hubble flow distance for galaxies outside HCG 44 (29 and 24 Mpc for SDSS J1017 and UGC 05574, respectively – see Table 1).
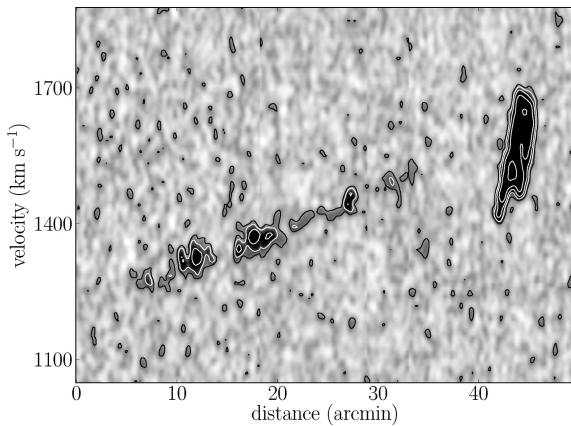
Figure 4. Position–velocity diagram of the H I emission along the path shown by the black solid line in Fig. 3. The origin of the horizontal axis is set to be at the northern end of the path. The bright emission at distance ~45 arcmin is H I in NGC 3187.
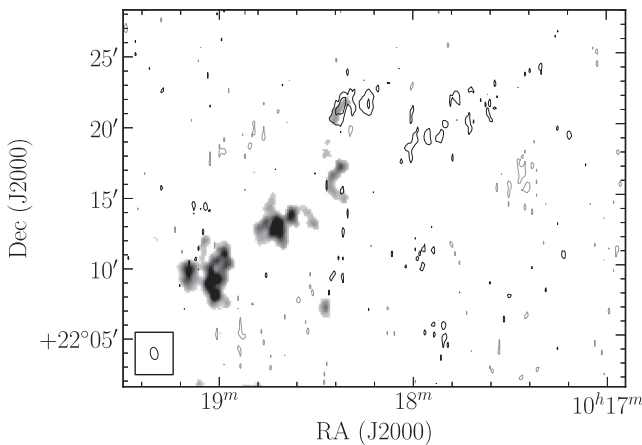
Figure 5. Contours of the H I emission in the natural-weighting cube at a recessional velocity of 1248 km s^{-1} overlaid on a grey-scale total-H I image of part of the tail T_N. Grey contours are at -0.4 mJy beam^{-1}, black contours at $+0.4$ and $+0.8$ mJy beam^{-1}. The figure shows possible additional emission north-west of T_N. Note that this low-level emission was not cleaned (i.e. it was not deconvolved with the beam).

We note that the lower value of our M(H I) estimates compared to values in Williams et al. (1991) would imply an even larger H I deficiency than that derived by Verdes-Montenegro et al. (2001) (see Section 2). We revisit the H I deficiency of galaxies in HCG 44 using the relation between M(H I) and optical diameter $D_{25,r}$ derived by Toribio et al. (2011). The isophotal major axis of NGC 3185, NGC 3187 and NGC 3190 is given in the SDSS Data Release 7 (DR7) catalogue and is 8.7, 6.5 and 13.4 kpc, respectively. Given these values, the H I mass predicted by the $1/V_{max}$-corrected M(H I)–$D_{25,r}$ relation in Toribio et al. (2011) is 7.8, 5.4 and 13.5×10^9 M$_\odot$, respectively. Therefore, the detected mass of H I is just 4, 22 and 4 per cent of the expected value for the three galaxies (6σ, 3σ and 6σ below the expected H I mass, respectively, where $\sigma = 0.23$ dex is the rms residual of Toribio et al. 2011 relation).

5 DISCUSSION

The detection of a 300-kpc-long tail containing 5×10^8 M$_\odot$ of H I in a group already observed by various authors with many different radio telescopes may seem surprising (see Section 2 for a summary of previous H I observations of HCG 44). Our result demonstrates that signatures of *ongoing* galaxy evolution inside groups can be truly elusive. It shows that although H I observations are unique in giving direct evidence of the fundamental role of group processes for galaxy evolution (as shown not only on individual systems but also on large, statistically representative samples; e.g. Serra et al. 2012), such observations need to be very sensitive and cover a large field if we want to gather a complete census of these events. This should be kept in mind when designing future H I surveys.

Besides the above general conclusion, our observations reveal for the first time direct evidence of gas stripping in HCG 44. This is interesting because galaxies in this group have long been known to be H I deficient and we may be unveiling the cause of at least part of the deficiency. It is therefore interesting to speculate on how the detected H I tail may have formed. How was the gas stripped, and from what galaxy? The goal of the present section is to explore possible answers to these two questions.

5.1 Formation of the H I tail: ram pressure or tidal stripping

The two possible mechanisms to form a gas tail within a group are ram pressure and tidal stripping. The former necessitates a dense medium and large relative velocity between the medium and the stripped galaxy. So far, X-ray observations have been unsuccessful in detecting the intragroup medium of HCG 44 (Mulchaey et al. 2003 using *ROSAT* data; Rasmussen et al. 2008 using *Chandra* and *XMM–Newton* data). Rasmussen et al. (2008) estimate that the density of the medium is $n < 10^{-4}$ cm^{-3}. Analytic calculations indicate that even at such low density some stripping might occur but they also show that this would be a fairly small effect (e.g. Rasmussen et al. 2008; Freeland, Sengupta & Croston 2010; Westmeier, Braun & Koribalski 2011). It therefore seems unlikely that ram pressure is responsible for creating such a prominent tail, longer than and as massive as tails detected in the centre of clusters (e.g. Oosterloo & van Gorkom 2005). Furthermore, no galaxy in the group shows the typical H I morphology caused by ram-pressure stripping – i.e. gas compressed against the stellar disc on one side of the galaxy and extending to larger radius on the opposite side (e.g. Kenney, van Gorkom & Vollmer 2004; Chung et al. 2007, 2009). We conclude that ram pressure is an unlikely explanation for the formation of T_N.

The alternative hypothesis is that T_N was created by tidal interaction within the group. Tidal forces act on both stars and gas and it
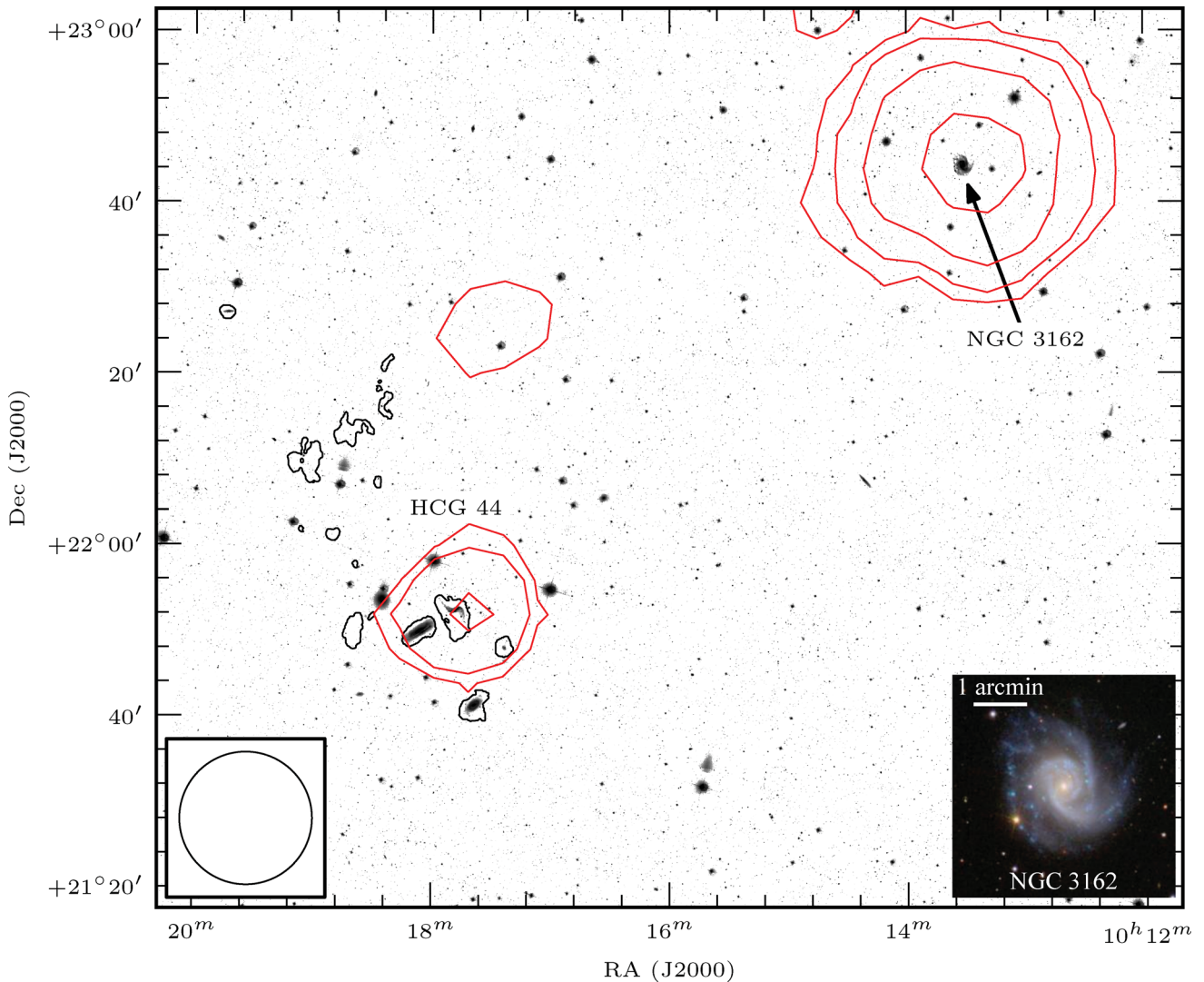
Figure 6. HIPASS (red) and WSRT (black) H I contours on top of a SDSS g-band image. We show the HIPASS beam (15.5 arcmin) in the bottom-left corner. HIPASS contours are drawn at $N(\text{H I}) = 1.0 \times 10^{18} \times 3^{n}$ cm^{-2} ($n = 0, 1, 2, 3$). The WSRT contour is the lowest contour shown in Fig. 2: 1.0×10^{19} cm^{-2}. The bottom-right inset shows the SDSS optical colour image of NGC 3162 obtained at http://skyserver.sdss3.org/dr8/en/tools/chart/chart.asp.

may therefore seem surprising that no diffuse stellar light is detected at the location of T_{N} even in the very deep CFHT/MegaCam image shown in Fig. 2. In fact, observations (e.g. Davies et al. 2004) and simulations (e.g. Bekki et al. 2005; Duc & Bournaud 2008; Michel-Dansac et al. 2010) both show that starless tidal tails can develop following gravitational interaction and depending on the relative distribution of gas and stars in the stripped galaxy. Therefore, tidal interaction is a viable mechanism to create the detected tail and we explore this possibility in the rest of this section.

5.2 What stripped galaxy?

The first question we attempt to answer is what galaxy the H I was stripped from. The results described in Section 4 suggest two alternative hypotheses. One possibility is that the tail was stripped from NGC 3162 as it flew by the group at high speed (see Fig. 6). This galaxy is currently at a projected distance of ∼650 kpc from HCG 44, which it could have covered in ∼3 Gyr if it went through the group at a velocity of 200 km s^{-1} on the plane of the sky. The optical morphology of this galaxy may support this hypothesis as the

stellar disc is lopsided, indicating that it might have been perturbed recently (see inset in Fig. 6). However, lopsidedness is a relatively common phenomenon in spiral galaxies and is no definite proof of an interaction between NGC 3162 and HCG 44. The newly reduced HIPASS data (Calabretta et al., in preparation) hint to a possible H I bridge between T_{N} and NGC 3162 which, if confirmed, would be a strong clue in favour of this hypothesis. This will be explored further in a future paper presenting the new data.

The other possibility is that the observed H I tail originated from one of the galaxies currently within HCG 44, and NGC 3162, played no significant role. Optical imaging shows that some of the members of HCG 44 have experienced recent tidal interaction (see Fig. 1), and T_{N} may have formed as part of the same process.

The most obvious candidate for tidal stripping within the group might be NGC 3187. This galaxy exhibits a strong tidal distortion visible as an S-shaped warp and T_{N} could be seen as an extension of the north-east side of the warp (see Fig. 2; note that any connection between T_{N} and NGC 3187 would have to be at column density below ∼10^{19} cm^{-2}). This is confirmed by the fact that the H I velocity on the south-west end of T_{N} is similar to that on the

north-east side of NGC 3187 (Figs 3 and 4). Another interesting point is that gas in T_N amounts to almost half of the total-H I mass of NGC 3187. Therefore, tidal stripping would provide a possible explanation for the H I deficiency of this galaxy (see Section 4.2). We speculate on the details of the stripping process below.

5.3 Tidal stripping of NGC 3187

Numerous previous authors argued that NGC 3187 might be interacting with NGC 3190. While this is possible, it is unlikely that such interaction is responsible for the formation of T_N. The reason is that it would be difficult to explain the gap between H I in NGC 3187 and T_N. Furthermore, compared to previously known cases of very long tails induced by ∼major galaxy interaction and merging (e.g. Mirabel, Lutz & Maza 1991; Duc et al. 2011), the length of the tail – at least 300 kpc – seems too extreme to be caused by this particular galaxy pair.

A mechanism to form very long, low-column-density H I tails (or rings) like that in HCG 44 was proposed by Bekki et al. (2005). The main ingredient of their model is the tidal interaction of a low-surface-brightness disc (in this case NGC 3187) with the gravitational potential of a group of galaxies. This interaction would strip the outer part of the disc (which are often observed to be essentially starless) and distribute the stripped material on a long tail or ring.

We perform a basic test of this mechanism and estimate the time-scale of the stripping process by building a 3D toy model for the orbit of NGC 3187 around HCG 44. The model is constrained by the assumed trajectory of NGC 3187 (traced by the H I tail and the current position of the galaxy) and its velocity relative to the group. In this model we assume the group potential to be fixed and Keplerian. We take the centre of the potential to be at the position of NGC 3193 and place it at coordinates $[x, y, z] = [0, 0, 0]$ (we discuss the orientation of the sky relative to these three axes below). We further assume that NGC 3187 follows a parabolic orbit parallel to the xy plane (and therefore at constant $z = z_0$).

For $z_0 = 0$ the orbit is determined only by the total mass of the system M_{tot} and the focal length of the parabola f. However, in this model we assume that the orbital plane is displaced relative to the centre of the group ($z_0 \neq 0$; we show below that this is necessary for the parabola to fit the data). Under this assumption NGC 3187 should move also along the z-axis but we neglect this effect. Such additional motion would be little constrained by the available data and would not in any case have a significant impact on the time-scale of the orbit, which is our primary goal. Therefore, the orbit remains perfectly planar (this approximation becomes increasingly wrong as the xy distance of NGC 3187 from the group centre gets closer to the value of z_0).

The toy model described above has only three free parameters: M_{tot}, f and z_0. We fix $M_{tot} = 5 \times 10^{12}$ M$_\odot$. We vary f between 50 and 200 kpc, and z_0 between 0 and 200 kpc in an attempt to reproduce the observations. Furthermore, in order to compare the model to the data we need to project it on the sky. This introduces additional degrees of freedom. We make use of 3D visualization to find a favourable projection.

Fig. 7 shows a possible orbit of NGC 3187, which reproduces the location of the H I tail and that of the galaxy at once. The orbit is obtained with $f = 75$ kpc and $z_0 = 100$ kpc, and is viewed at an inclination of 60° away from face-on (note that this is not the result of a formal fit and is therefore just one possible solution of the problem). An important feature of the model is that the predicted velocity of NGC 3187 relative to the group centre (i.e. NGC 3193) is 235 km s^{-1} along the line of sight. This is a good match to
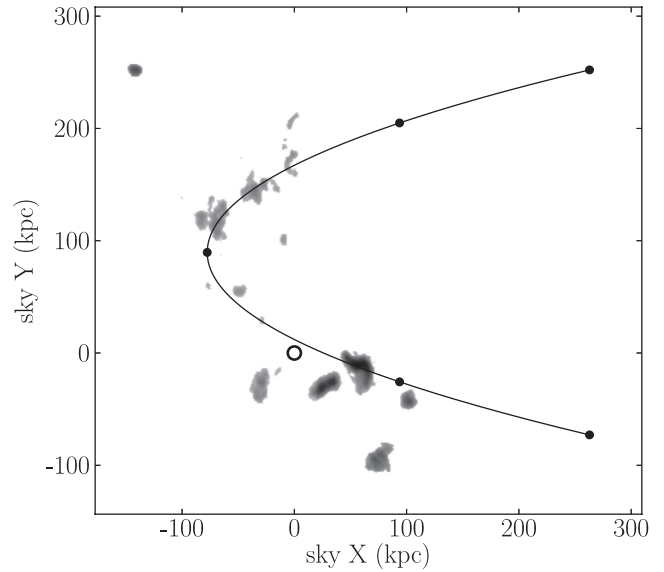

Figure 7. Total H I image of HCG 44 (logarithmic grey scale) with superimposed the possible orbit of NGC 3187 through the group (black line; see text). The open black circle indicates the position of NGC 3193, assumed centre of the group. Solid black circles are spaced at 0.5 Gyr time intervals.

the observed value of 210 km s^{-1} (see Table 1). Therefore, this simple model can explain the anomalous, high velocity of NGC 3187 relative to other members of HCG 44.

Within the context of this simple model NGC 3187 passed the vertex of the orbit ∼400 Myr ago and was at the current location of the north-west end of the H I tail (revealed by the HIPASS data shown in Fig. 6) ∼900 Myr ago. This suggests that the galaxy may have been stripped of the H I now in T_N (∼1/3 of its initial H I mass) within a time interval shorter than 1 Gyr. It is interesting that this time-scale is consistent with the ∼2 Gyr time-scale for quenching of star formation in galaxy groups recently derived by Rasmussen et al. (2012b).

There are some important differences between HCG 44 and the systems simulated by Bekki et al. (2005). First, their simulations predict the existence of a leading tail which, in the case of NGC 3187, should start at the southern tip of the warp, bend towards north-west and eventually join T_N to form an intragroup H I ring. This is not observed. Bekki et al. model is, however, an idealized one. In reality this process occurs in the presence of many other galaxies. It is possible that such second tail was destroyed by an interaction with NGC 3190 (which is tidally disturbed) and gas was instead dispersed towards the location of C_S. This idea is supported by both the H I and optical morphology of NGC 3187's southern tidal tail. Fig. 2 shows that this tail broadens and bends towards NGC 3190, giving support to the idea that the two galaxies are interacting. Therefore, it is possible that also gas in C_S once belonged to NGC 3187, and the above estimate on the amount of gas stripped from this galaxy should be regarded as a lower limit.

Another difference is that in Bekki et al. model the stripped galaxy is not tidally distorted, unlike NGC 3187. Again, interaction with NGC 3190 may explain the difference (note that, as we have argued above, this interaction is unlikely to be the formation mechanism of T_N itself).

We stress that we view this model as a very simple (but nevertheless useful) description of a possible formation mechanism for the detected tail. However, the system is complex: the group

membership is still to be established and a number of galaxies might be playing a relevant role, including the very distant NGC 3162 (see Fig. 6 and Section 5.2). As a consequence, substantial differences between the data and idealized simulations like that of Bekki et al. (2005) or simple models like the parabolic trajectory presented above are not a surprise. More detailed modelling is beyond the scope of this paper (for example, a realistic mass model of the group would be needed, and the line-of-sight velocity of gas in T_N should be used as a constraint for the model – taking into account also rotation within the stripped galaxy). Such modelling or the exploration of different formation mechanisms for the tail (e.g. interaction between NGC 3162 and a member of HCG 44 within the group potential, as in the models by Bekki, Koribalski & Kilborn 2005) would strongly benefit from having deep H I observations over a larger field.

6 CONCLUSIONS

We have presented deep H I and optical imaging of the galaxy group HCG 44 obtained with the WSRT and CFHT/MegaCam, respectively, as part of the ATLAS³ᴰ project. We detect a long intragroup H I tail and additional intragroup gas which, together, amount to 20 per cent of the H I mass of the group. Combining these data with archive HIPASS observations we find that the main tail contains $\sim 5 \times 10^8$ M$_\odot$ of H I and is $\sim$300 kpc long assuming a distance of 25 Mpc. The tail has no diffuse optical counterpart down to $\sim$28.5 mag arcsec^{-2} in g band.

We discuss viable formation mechanisms for the H I tail. Based on the available data (including X-ray imaging), it is unlikely that the tail is caused by ram-pressure stripping. Instead, it is possible that the H I was stripped from NGC 3187, a member of HCG 44, by the group tidal field. We present a simple model for the orbit of the stripped galaxy through the group. Within this model, NGC 3187 has been stripped of 1/3 of its initial gas mass in less than 1 Gyr. This is consistent with recent estimates of the time-scale for quenching of star formation in galaxy groups ($\sim$2 Gyr).

The proposed model is intentionally simple and it is possible that other processes have contributed to shaping the properties of galaxies in the group (e.g. tidal interaction between group members and, possibly, some ram-pressure stripping). Another possibility suggested by HIPASS data is that H I in the tail was stripped from NGC 3162, a spiral galaxy now 650 kpc from the group. Future work will investigate this possibility using H I data of better quality than those available at the moment.

Regardless of the precise formation mechanism, the detected H I tail is the first, direct evidence of gas stripping in HCG 44, a group long known to be deficient of H I. Our result highlights the importance of group processing as a driver of galaxy evolution, but also the observational challenge that has to be overcome in order to detect signatures of these processes. Sensitive H I observations over a large field are needed to gather a complete census of this kind of events in the local Universe.

REFERENCES

Aguerri J. A. L., Castro-Rodríguez N., Napolitano N., Arnaboldi M., Gerhard O., 2006, A&A, 457, 771
Amanullah R. et al., 2010, ApJ, 716, 712
Barnes D. G. et al., 2001, MNRAS, 322, 486
Bekki K., Couch W. J., 2011, MNRAS, 415, 1783
Bekki K., Koribalski B. S., Ryder S. D., Couch W. J., 2005, MNRAS, 357, L21
Bekki K., Koribalski B. S., Kilborn V. A., 2005, MNRAS, 363, L21
Blakeslee J. P., Lucey J. R., Barris B. J., Hudson M. J., Tonry J. L., 2001, MNRAS, 327, 1004
Borthakur S., Yun M. S., Verdes-Montenegro L., 2010, ApJ, 710, 385
Cappellari M. et al., 2011a, MNRAS, 413, 813
Cappellari M. et al., 2011b, MNRAS, 416, 1680
Chung A., van Gorkom J. H., Kenney J. D. P., Vollmer B., 2007, ApJ, 659, L115
Chung A., van Gorkom J. H., Kenney J. D. P., Crowl H., Vollmer B., 2009, AJ, 138, 1741
Davies J. et al., 2004, MNRAS, 349, 922
Dressler A., 1980, ApJ, 236, 351
Duc P.-A., Bournaud F., 2008, ApJ, 673, 787
Duc P.-A. et al., 2011, MNRAS, 417, 863
Elias-Rosa N. et al., 2008, MNRAS, 384, 107
English J., Koribalski B., Bland-Hawthorn J., Freeman K. C., McCain C. F., 2010, AJ, 139, 102
Freeland E., Stilp A., Wilcots E., 2009, AJ, 138, 295
Freeland E., Sengupta C., Croston J. H., 2010, MNRAS, 409, 1518
Garcia A. M., 1993, A&AS, 100, 47

Geller M. J., Huchra J. P., 1983, ApJS, 52, 61

Hibbard J. E., van Gorkom J. H., Rupen M. P., Schiminovich D., 2001, inHibbard J. E., Rupen M., van Gorkom J. H., eds, ASP Conf. Ser. Vol. 240, Gas and Galaxy Evolution. Astron. Soc. Pac., San Francisco, p. 657

Hickson P., 1982, ApJ, 255, 382

Kenney J. D. P., van Gorkom J. H., Vollmer B., 2004, AJ, 127, 3361

Kern K. M., Kilborn V. A., Forbes D. A., Koribalski B., 2008, MNRAS, 384, 305

Kilborn V. A., Forbes D. A., Barnes D. G., Koribalski B. S., Brough S., Kern K., 2009, MNRAS, 400, 1962

Koribalski B. S., López-Sánchez Á. R., 2009, MNRAS, 400, 1749

Koribalski B., Gordon S., Jones K., 2003, MNRAS, 339, 1203

Kreckel K., Platen E., Aragón-Calvo M. A., van Gorkom J. H., van de Weygaert R., van der Hulst J. M., Beygu B., 2012, AJ, 144, 16

Krumm N., Burstein D., 1984, AJ, 89, 1319

Mandel K. S., Wood-Vasey W. M., Friedman A. S., Kirshner R. P., 2009, ApJ, 704, 629

Meurer G. R., Carignan C., Beaulieu S. F., Freeman K. C., 1996, AJ, 111, 1551

Michel-Dansac L. et al., 2010, ApJ, 717, L143

Mirabel I. F., Lutz D., Maza J., 1991, A&A, 243, 367

Morganti R. et al., 2006, MNRAS, 371, 157

Mulchaey J. S., Davis D. S., Mushotzky R. F., Burstein D., 2003, ApJS, 145, 39

Oosterloo T., van Gorkom J., 2005, A&A, 437, L19

Oosterloo T. A., Morganti R., Sadler E. M., van der Hulst T., Serra P., 2007, A&A, 465, 787

Postman M., Geller M. J., 1984, ApJ, 281, 95

Rasmussen J., Ponman T. J., Verdes-Montenegro L., Yun M. S., Borthakur S., 2008, MNRAS, 388, 1245

Rasmussen J. et al., 2012a, ApJ, 747, 31

Rasmussen J., Mulchaey J. S., Bai L., Ponman T. J., Raychaudhury S., Dariush A., 2012b, ApJ, 757, 122

Reindl B., Tammann G. A., Sandage A., Saha A., 2005, ApJ, 624, 532

Sancisi R., Fraternali F., Oosterloo T., van der Hulst T., 2008, A&AR, 15, 189

Schiminovich D., van Gorkom J. H., van der Hulst J. M., Kasow S., 1994, ApJ, 423, L101

Schneider S. E., Helou G., Salpeter E. E., Terzian Y., 1983, ApJ, 273, L1

Scott T. C., Cortese L., Brinks E., Bravo-Alfaro H., Auld R., Minchin R., 2012, MNRAS, 419, L19

Serra P. et al., 2012, MNRAS, 422, 1835

Springob C. M., Masters K. L., Haynes M. P., Giovanelli R., Marinoni C., 2009, ApJS, 182, 474

Szomoru A., van Gorkom J. H., Gregg M. D., Strauss M. A., 1996, AJ, 111, 2150

Takanashi N., Doi M., Yasuda N., 2008, MNRAS, 389, 1577

Thilker D. A. et al., 2009, Nat, 457, 990

Toribio M. C., Solanes J. M., Giovanelli R., Haynes M. P., Martin A. M., 2011, ApJ, 732, 93

Tully R. B., 1988, Nearby Galaxies Catalog. Cambridge Univ. Press, Cambridge

van der Hulst J. M., 1979, A&A, 75, 97

van Driel W., van Woerden H., 1991, A&A, 243, 71

van Driel W., Marcum P., Gallagher J. S., III, Wilcots E., Guidoux C., Monnier Ragaigne D., 2001, A&A, 378, 370

Verdes-Montenegro L., Yun M. S., Williams B. A., Huchtmeier W. K., Del Olmo A., Perea J., 2001, A&A, 377, 812

Verheijen M. A. W., Zwaan M., 2001, inHibbard J. E., Rupen M., van Gorkom J. H., eds, ASP Conf. Ser. Vol. 240, Gas and Galaxy Evolution. Astron. Soc. Pac., San Francisco, p. 867

Vorontsov-Velyaminov B. A., 1959, Atlas and Catalog of Interacting Galaxies. Moscow State University

Wang X., Wang L., Pain R., Zhou X., Li Z., 2006, ApJ, 645, 488

Westmeier T., Braun R., Koribalski B. S., 2011, MNRAS, 410, 2217

Williams B. A., Rood H. J., 1987, ApJS, 63, 265

Williams B. A., McMahon P. M., van Gorkom J. H., 1991, AJ, 101, 1957

Wilman D. J., Oemler A., Jr, Mulchaey J. S., McGee S. L., Balogh M. L., Bower R. G., 2009, ApJ, 692, 298

Wong O. I. et al., 2006, MNRAS, 371, 1855

Wood-Vasey W. M. et al., 2008, ApJ, 689, 377

This paper has been typeset from a TeX/LaTeX file prepared by the author.